Differentiating Acute Otitis Media (AOM) from Otitis Media with Effusion (OME) Using Autofluorescence of NADPH in Neutrophils

By:
Caroline V. Anderson, Layth A. Popp, Esha Tulsian and Dreyden E. Wedertz

Word Count: 3,449
Number of Figures/Tables: 6
Number of Equations: 3
Number of Supplements: 5
Number of References: 24

Advisor: Dr. William Guilford, Department of Biomedical Engineering

Advisor Signature: 

Differentiating Acute Otitis Media (AOM) from Otitis Media with Effusion (OME) Using Autofluorescence of NADPH in Neutrophils

Caroline V. Anderson[a], Layth A. Popp[a], Esha Tulsian[a], Dreyden E. Wedertz[a], William H. Guilford[a]

[a]Department of Biomedical Engineering, University of Virginia, Charlottesville, VA

Abstract

Eighty to ninety percent of children will be diagnosed with otitis media (OM) - also known as an ear inflammation - before reaching school age. There are two subtypes of OM: acute otitis media (AOM) and otitis media with effusion (OME). AOM is an accumulation of middle ear fluid (MEF) due to viral or bacterial pathogens leading to the recruitment of neutrophils. OME is due to a mechanical malfunction of the eustachian tubes. Currently, pediatricians face a 50% misdiagnosis rate of OM type. This is of concern due to the different treatment approaches. While AOM is resolved with antibiotics, OME requires surgical drainage of MEF. We have developed a diagnostic method for measuring neutrophil autofluorescence levels to differentiate between AOM and OME to address the high rate of OM type misdiagnosis among pediatricians. An excitation light of 360 nm was emitted from an LED, filtered through a dichroic mirror, and focused through a lens onto a NADPH sample. Light emitted from the sample was collected by a lens and re-imaged onto a photomultiplier tube (PMT) after passing through a lens and emission filter. The PMT output current was amplified and converted to an output voltage by a transimpedance amplifier, which was measured by a LabVIEW virtual instrument. Two-fold direct dilutions from an NADPH stock solution were performed. Results suggest the instrument is sensitive for detecting NADPH concentrations down to 1.17 μM. The current instrument is not sensitive for detecting physiologically relevant concentrations of NADPH associated with AOM and OME. Future work seeks to increase instrument sensitivity for detecting these concentrations.

Keywords: otitis media, NADPH, autofluorescence, acute otitis media, otitis media with effusion

---

Introduction

Clinical Background

Otitis media (OM), or middle ear inflammation, is one of the most common childhood illnesses and a leading cause of conductive hearing loss in children[1,2]. Eighty to ninety percent of children will be diagnosed with OM before reaching school age[3]. Hearing loss can impact children in numerous ways, including delaying speech development, stunting acquisition of social skills, and negatively affecting academic performance[4]. Two of the subtypes of OM are common in children: acute otitis media (AOM) and otitis media with effusion (OME)[1]. AOM is a bacterial or viral infection of accumulated middle ear fluid (MEF), while OME presents as a non-infectious accumulation of MEF behind the tympanic membrane[1].

Clinical Problem

There is a 50% misdiagnosis rate of OM type among pediatricians[5,6]. This is of concern due to the difference in treatment each condition necessitates[1]. AOM is treatable with antibiotics, while OME is unresponsive to antibiotics and may require surgical drainage of MEF[1]. Misdiagnosing OM type can have serious consequences for patients and their families. A misdiagnosis of OM type results in pediatricians recommending the incorrect

treatment to patients. Such inaccurate medical interventions can lead to unnecessary antibiotic usage, chronic OM, prolonged patient discomfort, and increased total cost of OM medical care, which is already currently estimated at $4.3 billion annually in the United States[7].

Current Diagnostic Methods

The otoscope is currently the most popular diagnostic device for middle ear dysfunctions, including OM. Using lighting and magnification, the otoscope allows clinicians to observe the middle ear space and make diagnoses based upon the appearance of the tympanic membrane. However, there are imperfections in this approach. While otoscopes are highly practical and intuitive to use, the indistinct appearance of the tympanic membrane complicates the accuracy of differentiation between AOM and OME by observation alone. This limitation contributes to the high rates of OM type misdiagnosis among clinicians[5]. Using an otoscope, otolaryngologists and pediatricians both misdiagnose OM type; however, pediatricians were found to misdiagnose OM type at a higher rate than otolaryngologists[5]. Pediatricians who rely on otoscopes to diagnose OM type overdiagnose AOM 27% of the time compared to 24% among otolaryngologists[5].

A few alternative diagnostic tools to otoscopes currently exist. Pediatric clinicians could more accurately differentiate between AOM and OME through tympanocentesis[5]. Tympanocentesis is a diagnostic technique that involves the surgical drainage of MEF from the tympanic membrane, so that the extracted fluid can be tested for infection[5]. While an accurate diagnosis of OM could be obtained through such procedures, tympanocentesis is an impractical first-line diagnostic method due to its highly invasive nature[5]. Therefore, the development of a non-invasive diagnostic method to accurately differentiate between AOM and OME is of interest. Such an instrument would reduce the rates of OM type misdiagnosis among pediatric clinicians.

Researchers have investigated methods to improve upon the limitations of the traditional otoscopes for accurately diagnosing middle ear pathologies. A team at Johns Hopkins University and the University of Maryland developed OtoPhoto, an otoscope that uses AI to diagnose pediatric ear pathologies[8]. OtoPhoto consists of three components: an AI-based algorithm that can diagnose pathologies based on video, a digital otoscope that can capture the ear and have capability for high-quality ear exams, and an application that can record and communicate data. The team emphasized that this device is easy to use by anyone and is quick in diagnosing whether an ear infection is present.

Another group of researchers designed a terahertz (THz) otoscope to diagnose OM[9]. THz electromagnetic waves are sensitive to biomolecules and water, so the research team used this to assess the presence of pus that is associated with infectious OM types. The team had a successful design, but their design was limited by the technology's sensitivity to membrane geometry.

Proposed Diagnostic Method

The proposed diagnostic method differs from previous innovations through its reliance on a measurable biomarker for the non-invasive diagnosis of middle ear pathologies. During an infectious accumulation of MEF, various white blood cells (WBCs) migrate to inflamed regions to neutralize pathogens as part of an innate immune response. Several WBCs migrate to such regions to combat infection, including neutrophils[10]. The role of neutrophils in the innate immune response to OM is of particular interest[10]. Neutrophils have been found at higher concentrations in AOM MEF than OME MEF and are known to contain NADPH, an autofluorescent molecule, at higher levels than other cell lineages[11–13]. NADPH is a product of the pentose phosphate pathway resulting from the reduction of NADP+ into NADPH[14]. NADPH oxidases (NOXs) use NADPH and other molecules to generate reactive oxygen species (ROS) to neutralize pathogens[15]. Given the high concentrations of neutrophils found in AOM MEF compared to OME MEF and autofluorescent nature of NADPH, this molecule represents a promising biomarker for the non-invasive differentiation of AOM and OME[11,12].

Project Hypotheses and Aims

Through the design of a diagnostic method that takes advantage of the autofluorescence of NADPH, we expect to establish instrument functionality and sensitivity for detecting NADPH in a free solution. Once established, we expect the differentiation of AOM and OME among clinicians is expected to increase in accuracy. Current diagnostic techniques are incapable of

accurately differentiating between an infected and non-infected fluid-filled ear. We believe the proposed diagnostic method using NADPH as an indicator of disease will lead to a reduction in misdiagnosed cases, unnecessary surgeries, and prescriptions. Once this method proves that NADPH can be used as a marker to detect concentrations of neutrophils, new research will develop in an attempt to reduce the size of the electronics and create a handheld device capable of this detection. Having a device capable of detecting elevated concentrations of neutrophils will allow physicians to make more accurate diagnoses.

We hypothesize that the detection of NADPH autofluorescence can be used to differentially diagnose AOM and OME. We developed the following aims to test this hypothesis. The first aim of this project was to verify in literature the concentrations of NADPH in the MEF of patients with AOM and OME. Concentrations of NADPH in neutrophils in suspension found in MEF for AOM and OME were estimated from literature to be $6.3*10^{-8}$ M and $3.3*10^{-9}$ M, respectively. One study found the concentration of NADPH within a singular neutrophil to be 50 μM[16], another established the volume of a singular neutrophil to be 600 μm^3 [17], and a third that in AOM middle ear fluid there are $2.11*10^{-6}$ neutrophils/mL MEF[12]. Multiplying these values together, along with the appropriate unit conversions, yielded an approximate NADPH concentration of $6.3*10^{-8}$ M in AOM MEF. Previous studies have also found that there is a 2.1:1 ratio of neutrophils to lymphocytes in OME MEF[11], there are $1.08*10^5$ lymphocytes per 1 mL of OME MEF[12]. In a suspension of neutrophils there is approximately 14.5 pmol of NADPH per 10^6 neutrophils[18]. Multiplying the OME pertinent values together and applying unit conversions, the NADPH concentration in OME MEF was estimated to be $3.3*10^{-9}$ M. The second aim of this project was to construct a diagnostic instrument capable of detecting NADPH autofluorescence. The final aim of this project was to demonstrate instrument functionality and sensitivity to detect physiologically-relevant concentrations of NADPH in free solution.

Design Constraints

A constraint in using NADPH as a biomarker is its low quantum efficiency, found to be about 0.019 or 2%[19]. Quantum efficiency is defined as the measure of a detector to effectively convert photons to electrons. This low efficiency posed a limitation in the instrument detecting NADPH. The instrument was also limited by the extinction coefficient of NADPH, which is 3300 L/mol-cm[20]. This coefficient, an intrinsic property of NADPH autofluorescence, details how strongly NADPH can absorb or reflect light at a particular wavelength. In addition, detection was constrained by the concentrations of NADPH found in AOM and OME MEF, which although elevated in comparison to healthy ears, is still exceedingly small.

Results

Instrument Functionality Established for Detecting NADPH in Free Solution

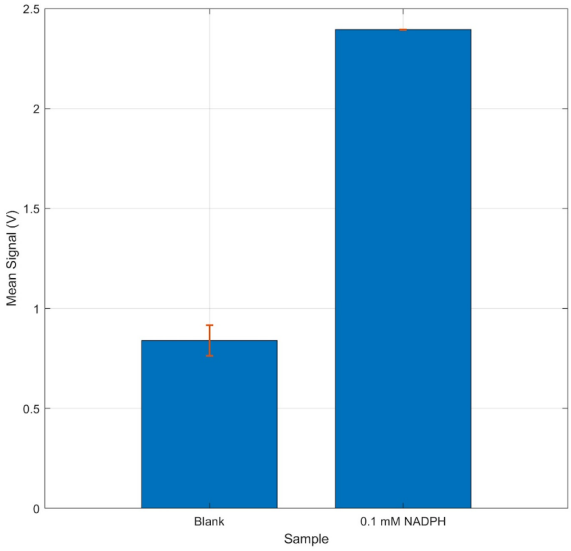

Figure 1: Mean Signal of 0.1 mM NADPH Stock Solution and Deionized Water Blank at 3.0 V Excitation Light and 0.6 V PMT Gain. *A barplot comparing the mean signal for a 0.1 mM stock solution of NADPH relative to background. A statistically significant difference in signal was determined from the results of an unpaired, two-sample z-test (p-value < 0.00001, two-tailed) at the 0.05 significance level.*

To establish instrument functionality for detecting NADPH concentrations above background, a 0.1 mM stock solution of NADPH was prepared alongside a blank solution of deionized water. Mean signals of 2.39 V and 0.84 V were measured from the NADPH stock solution and blank, respectively (Figure 1). Standard deviation for each sample was calculated for both samples and plotted as error bars. An unpaired, two-sample z-test was performed in MATLAB using the

signal measurements of both samples. A statistically significant difference between the stock solution and blank was identified at the 0.05 significance level, with a p-value < 0.0001 (two-tailed). These results indicate that the instrument is capable of detecting NADPH autofluorescence in free solution.

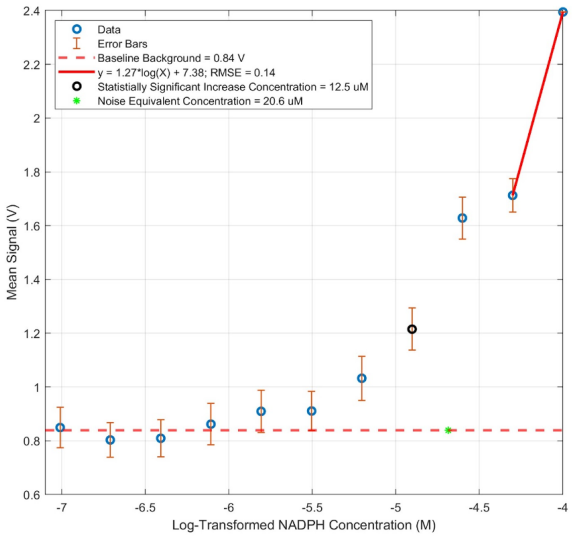

Figure 2: 2-Fold Direct Dilutions from 0.1 mM NADPH Stock Solution using Deionized Water Diluent at 3.0 V Excitation Light and 0.6 V PMT Gain. *The mean signal for NADPH samples ranging from 0.1 mM to 97.7 nM were plotted against log-transformed concentrations in molar units. The noise equivalent concentration was calculated from the intersection of the linear region with the dashed line denoting background.*

Performing 2-fold direct dilutions from a 0.1 mM NADPH stock solution down to 97.7 nM, a preliminary noise equivalent concentration was calculated (Figure 2). The noise equivalent concentration represents the NADPH concentration for which its fluorescence signal is equivalent to the background signal with no emitted light. This concentration of NADPH is thereby the lowest the instrument can detect. Mean signal for each dilution was plotted against log-transformed NADPH sample concentrations and analyzed in MATLAB. The standard deviation was calculated for each dilution and plotted as error bars.

An unpaired, two-sample z-test was performed in MATLAB, and 12.5 µM was found to be the first concentration for which there was a statistically significant increase in signal relative to background, with a p-value = 0.0006 (two-tailed), at the 0.05 significance level (Figure 2). The samples ranging in concentration from 0.1 mM to 0.05 mM were identified as the linear region, and a linear regression was performed. The equation of this regression was calculated using a signal equivalent to that of background, 0.84 V, and evaluated for the concentration, X. The preliminary noise equivalent concentration for NADPH in deionized water was thus found to be 20.6 µM (Figure 2). The results of this experiment suggest the noise equivalent concentration of the instrument is on the order of 10^{-6} M.

NADPH Autofluorescence Decreases with Time

NADPH is an unstable coenzyme under certain conditions. The stability of NADPH posed a constraint for testing the proposed diagnostic method. Researchers have investigated the role of pH, temperature, ionic strength, buffer composition on the degradation kinetics of NADPH, and it has been found that NADPH is most stable at alkaline pHs[21]. Specifically, the degradation of NADPH was observed to slow down at pHs above 7.5[21]. Although it is known that phosphate and acetate buffers can accelerate NADPH degradation, studies have shown concentrations of phosphate or acetate 0.1 M or less have a minimal effect on NADPH degradation[21]. To establish instrument sensitivity for detecting physiology-relevant concentrations of NADPH in free solution, the degradation kinetics of this coenzyme will need to be considered.

To stabilize NADPH in free solution, 2-fold direct dilutions were performed using a 0.1 M potassium phosphate buffer (pH = 8.0) diluent. Direct dilutions were prepared from a 0.01 mM NADPH stock solution down to 0.061 nM, and the time-course of NADPH autofluorescence was established (Figure 3). NADPH autofluorescence was expected to decrease over time due to photobleaching.

Raw signal data for 10, 5, and 2.5 µM NADPH samples were plotted against time (Figure 3a). Signal data for each of the 4, 10-second trials during the period when the light was turned on were visualized in MATLAB. The initial increases in signal at the beginning of each trial are potentially an artifact of the externally controlled power supply of the LED light source. The change in signal over time, ΔS, for each dilution was calculated in MATLAB for the 10 and 5 µM NADPH

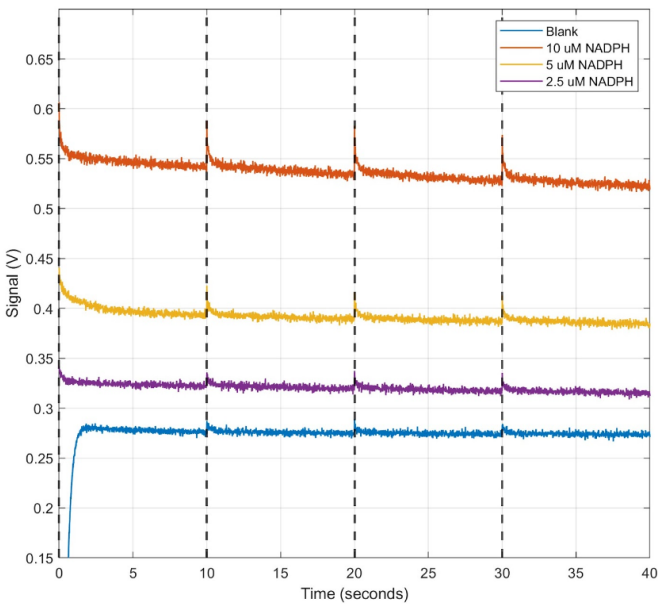

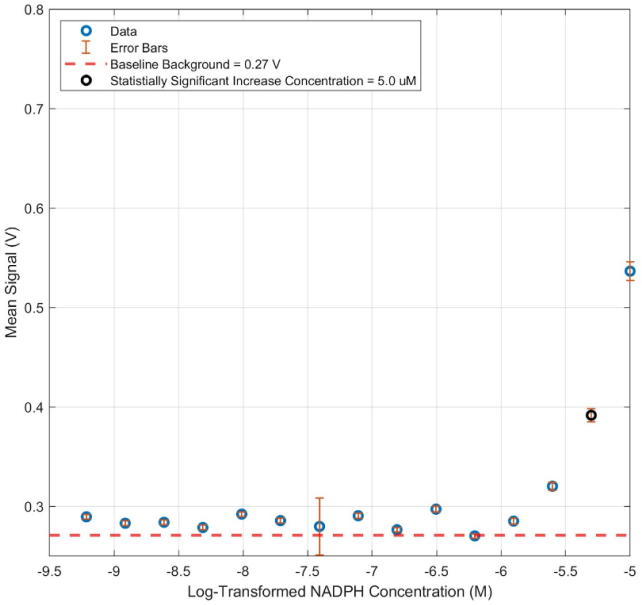

(A) ***(B)***

Figure 3: 2-Fold Direct Dilutions from 0.01 mM NADPH Stock Solutions using Potassium Phosphate Buffer Diluent at 3.0 V Excitation Light 0.6 V PMT Gain. (A) *The first panel shows a representative plot of the time-course of autofluorescence for 10, 5, and 2.5 uM NADPH samples relative to the potassium phosphate buffer blank. Dashed lines demarcate the start of a new 10-second period during which the light source is turned on.* ***(B)*** *The second panel shows the mean signal for NADPH samples ranging from 0.01 mM to 0.61 nM plotted against log-transformed concentrations in molar units.*

samples (Equation 1). The NADPH signal was found to decrease at a rate of 2.2 mV/second for the 10 µM sample and 1.4 mV/second for the 5 µM sample.

$$\Delta S = \frac{Signal_{Final} - Signal_{Start}}{Time_{Final} - Time_{Start}} \text{ (Equation 1)}$$

Mean signal for each dilution was plotted against log-transformed NADPH sample concentrations and analyzed in MATLAB (Figure 3b). Standard deviation was calculated for each sample and plotted as error bars. (Figure 3b). An unpaired, two-sample z-test performed in MATLAB identified 5 µM to the first statistically significant measurement above background, with a p-value = 0.0001 (two-tailed), at the 0.05 significance level. Not enough NADPH samples were above the statistically significant increase concentrations to perform a linear regression and calculate a noise equivalent concentration.

To establish the relationship between NADPH concentration and output signal, the difference in signal

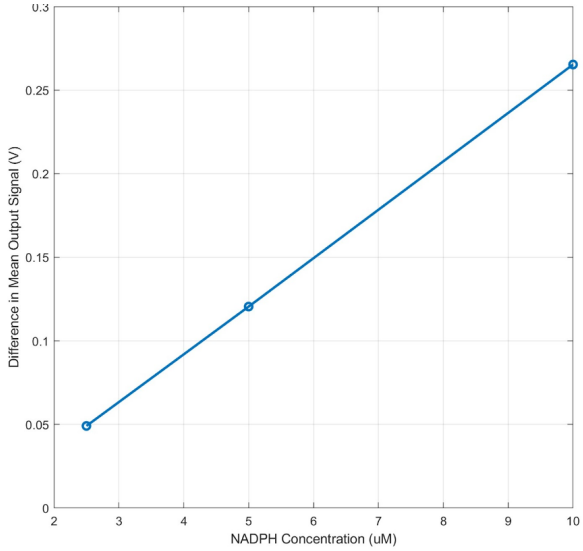

Figure 4: Difference in Mean Output Signal versus NADPH Concentration. *The differences in output signal between NADPH samples and the potassium phosphate buffer blank, ΔV, were plotted against NADPH concentration in MATLAB. The slope of the line was calculated using the equation k = [C]/ΔV, where k is the calibration factor of NADPH concentration per voltage and [C] is the change in NADPH concentration (µM). The calibration factor was found was found to be 34.69 µM/V.*

between that of NADPH samples and the potassium phosphate buffer blank, ΔV, was first computed for the 10, 5, and 2.5 µM NADPH samples (Equation 2). The difference in signal was calculated using the mean signal outputs of the NADPH samples and the blank.

$$\Delta V = \overline{Signal_{NADPH}} - \overline{Signal_{Blank}} \quad \text{(Equation 2)}$$

The difference in signal, ΔV, for the 10, 5, and 2.5 µM NADPH samples was calculated to be 0.27 V, 0.12V, and 0.05V, respectively. These differences in signal were then plotted against NADPH concentration and visualized in MATLAB (Figure 4). The slope of the linear relationship between ΔV and NADPH concentration was calculated to determine the calibration factor between NADPH concentration and output signal. This factor was found to be 34.67 µM/V.

Establishing Instrument Sensitivity for Detecting NADPH Down to 1.17 µM

To increase instrument sensitivity for detecting low concentrations of NADPH, PMT gain was increased to 0.7 V. Establishment of the optimal excitation light and PMT gain settings suggested that an excitation light of 3.0 V and PMT gain of 0.7 V would yield greater instrument sensitivity, using more of the instrument's dynamic range (S4). 2-fold direct dilutions from a 0.1 mM NADPH stock solution down to 0.61 nM were prepared using potassium phosphate buffer as the diluent diluent. From the results of this experiment the time-course of NADPH autofluorescence and noise equivalent concentration were established (Figure 5).

Raw signal data for 50 µM was plotted against time to observe the representative change in NADPH autofluorescence over time (Figure 5a). Signal data for each of the 4, 5-second trials during the period when the

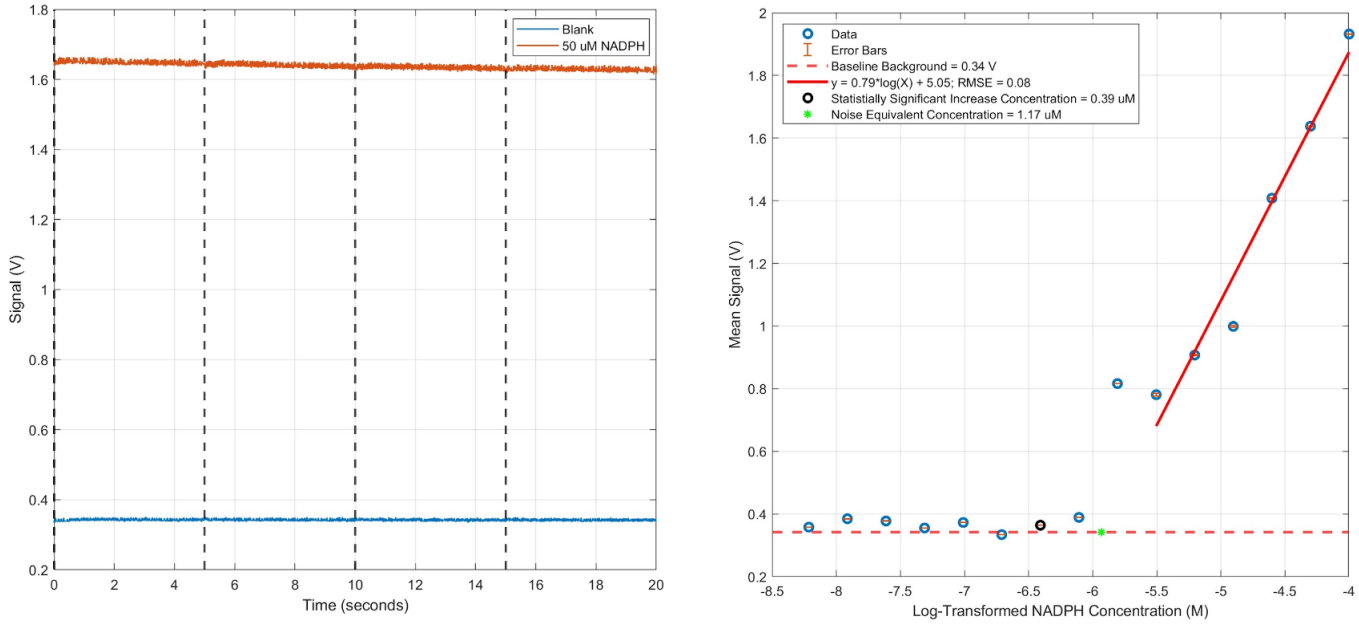

(A) ***(B)***

Figure 5: 2-Fold Direct Dilutions from 0.01 mM NADPH Stock Solutions using Potassium Phosphate Buffer Diluent at 3.0 V Excitation Light 0.7 V PMT Gain. ***(A)*** *The first panel shows a representative plot of the time-course of autofluorescence for 10, 5, and 2.5 uM NADPH samples relative to the potassium phosphate buffer blank. Dashed lines demarcate the start of a new 5-second period during which the light source is turned on.* ***(B)*** *The second panel shows the mean signal for NADPH samples ranging from 0.01 mM to 0.61 nM plotted against log-transformed concentrations in molar units. The noise equivalent concentration was calculated from the intersection of the linear region with the dashed line denoting background.*

light was turned on was visualized in MATLAB. Signal for this sample was observed to decrease in time, aligning from previous results assessing the time-course of NADPH autofluorescence. The change in signal over time, ΔS, for this 50 μM NADPH sample was calculated in MATLAB (Equation 1) and found to be 34.5 μV/second.

Mean signal for each dilution was plotted against log-transformed NADPH sample concentrations and analyzed in MATLAB (Figure 5b). Standard deviation was calculated for each dilution and plotted as error bars. The results of an unpaired, two-sample z-test found 0.39 μM be the first concentration for which there was a statistically significant increase in signal relative to background, with a p-value = 0.000013 (two-tailed), at the 0.05 significance level (Figure 5b). The samples ranging in concentration from 0.1 mM to 3.13 μM were identified as the linear region, and a linear regression was performed. The equation of this regression was evaluated using a signal equivalent to a background of 0.37 V. The equation was solved for concentration, X, and a noise equivalent concentration of 1.17 μM was calculated (Figure 5b). These results suggest the instrument is sensitive enough to detect NADPH down to a concentration of 1.17 μM.

Discussion

Though the PMT was sensitive enough to detect low NADPH concentrations in free solution, the instrument is not sensitive enough to detect physiologically-relevant NADPH concentrations in MEF of patients with AOM and OME. The instrument was sensitive enough to detect a concentration of about 1.17 uM, but the physiological concentrations are on the order of 10^{-8} M and 10^{-9} M for AOM and OME, respectively. NADPH autofluorescence was found to change over time by 2.2 mV/second for the 10 μM sample and 1.4 mV/second for the 5 μM sample. This calculation was necessary to understand the effect of photobleaching on NADPH.

Experimental Limitations

Several limitations may have precluded detection of physiologically-relevant NADPH concentrations. One limitation is the persistence of a moderate background signal. Although the background was reduced by switching to a glass cuvette, the background was not able to be lowered below 0.37 V. This may be due to ambient light from within the lab, light scattering, or limitations in the detection equipment utilized. A high background may obscure low voltage signals, resulting in an elevated noise equivalent concentration.

Additionally, the pH and composition of the chosen diluent, potassium phosphate, placed constraints on the precision of the system. The stability of NADPH is highly dependent on pH, with recommendations from manufacturers being that solutions be made at a pH of 8.0[22]. However, previous studies have found the pH of middle ear fluid to be approximately 7.86[23]. Thus, choosing to prioritize NADPH stability in the interest of assessing instrument capability sacrificed some physiological accuracy. NADPH degradation is also accelerated by high concentrations of phosphate. While literature suggests that concentrations below 100 mM have marginal effects on NADPH degradation, the phosphate may also have been a factor in the suboptimal NEC.

Finally, the experiment was conducted in an open air environment with atmospheric oxygen concentrations. Studies of the middle ear have found the space behind the middle ear to have an oxygen content of 5.66%, while atmospheric air is approximately 21% oxygen[24]. It is known that oxygen in the air photobleaches light, which could reduce the signal received by the PMT.

Future Directions

To improve the sensitivity of the instrument, the first goal will be to reduce background light. An excitation filter that only passes light between 360 nm to 370 nm of light could be used. This filter will ensure the light going through is mostly just the wavelength of light that will excite the NADPH, omitting any other wavelength of light. Fully encasing the instrument would also reduce background light and improve sensitivity. Additionally, the experiments would be repeated in low oxygen concentrations. This goal could be achieved in two ways. The free solution of NADPH could either be bubbled with nitrogen or argon gas or be integrated with an oxygen-scavenging system using glucose, glucose oxidase, and catalase. Lowering oxygen concentration would mimic the environment of the middle ear better and improve the sensitivity of the instrument through the minimization of photobleaching. Photobleaching may also be minimized through shortening the time periods

for data acquisition. All experiments were conducted with data acquisition times of 5 to 10 seconds per trial, or period when the light source was turned on.

Once the instrument is sensitive enough to detect the physiologically-relevant concentrations of about 10^{-8} and 10^{-9} M of NADPH, the goal would be to investigate NADPH detection in neutrophil suspensions. If this testing also is successful, the instrument would be tested on a phantom model, mimicking the tympanic membrane.

Materials & Methods

Diagnostic Instrument Design

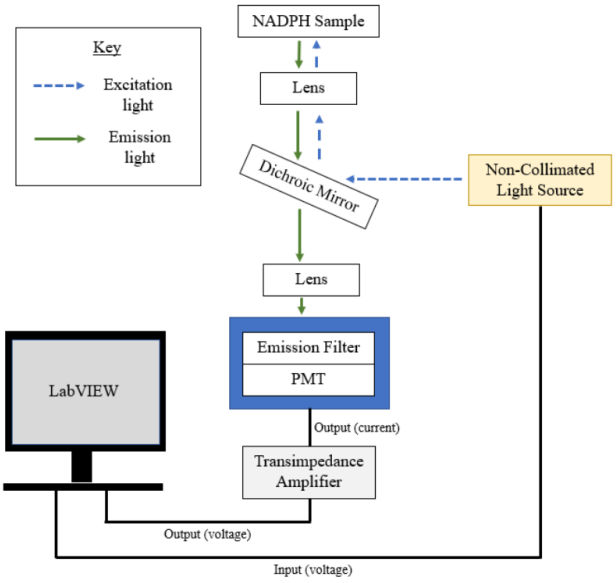

Figure 6: Design of Diagnostic Instrument. *The above schematic illustrates the relative placement of each component of the instrument and the path of both excitation and emission wavelengths through the instrument.*

A diagnostic instrument (Figure 6) was constructed to shine an excitation wavelength (~365 nm) from a non-collimated light source (LED, 365 nm, 0.88 W, ThorLabs). The excitation light was reflected off a dichroic mirror (325-404 nm reflection, 415-850 nm transmission) and imaged onto a cuvette containing an NADPH sample by a 7.3 mm focal length lens (ThorLabs). The emitted light from the NADPH sample was collected by the lens and was re-imaged onto a photomultiplier tube (PMT, Hamamatsu H10721-110, Edmund Optics) by a 25 mm focal length lens (ThorLabs) passing also through an emission filter (~425 nm). Next, a transimpedance amplifier (AMP102, ThorLabs) amplified and converted the current output from the PMT into a voltage output. A LabVIEW virtual instrument was created to control excitation light and PMT gain. The virtual instrument also collected and measured data from the PMT. Custom holders for the PMT and emission filter were designed in AutoCAD Fusion 360 and 3D-printed using black polylactic acid (PLA) (S1). Another custom holder to hold a glass cuvette was designed in AutoCAD Fusion 360 and 3D printed using black polylactic acid (PLA) (S2).

Expected power outputs for the proposed instrument were calculated using Equation 2, where $Power_{in}$ is the power applied to the instrument by the light source, $Power_{out}$ is the power received by the lens, c is NADPH concentration, ε is the extinction coefficient of NADPH as a fluorophore, QE is the quantum efficiency of NADPH as a fluorophore, $l_{cuvette}$ is the length of the cuvette, r_{lens} is the radius of the lens, and FL is the focal length of the lens. The term $\frac{r_{lens}^{\ 2}}{4*(FL)^2}$ refers to the fraction of light that is collected by the lens (Equation 3). These parameters reflect a combination of values from literature, and values measured directly from instrument components. $Power_{in}$ is 0.33 W, ε is 3300 L/mol*cm, $l_{cuvette}$ is 1 cm, QE is 0.019, r_{lens} is 25 mm, and FL is 7.3 mm.

The expected power output of the instrument was maximized through choice of lens diameter and focal length. In doing so, an optimal lens diameter and focal length pair were identified that would maximize the power output for NADPH autofluorescence detection. A 25 mm diameter lens with 7.3mm focal length was used to increase instrument sensitivity.

$$Power_{out} = \left[Power_{in} * \varepsilon * l_{cuvette} * QE * \frac{r_{lens}^{\ 2}}{4*(FL)^2}\right] * c$$

(Equation 3)

NADPH Tetrasodium Salt

100 mg of NADPH tetrasodium salt (97% dry weight) was purchased from Millipore Sigma (CAS Number: 2626-71-1, MDL Number: MFCD00036263, PubChem Substance ID: 329818701)[22]. The molecular weight of this product was 833.35 g/mol[22].

Potassium Phosphate Buffer

To stabilize NADPH in free solution, a 0.1 M potassium phosphate buffer (pH = 8.0) was created. To create the buffer, 800 mL of deionized water was prepared in a 1 L beaker. 16.28 g of dibasic potassium phosphate was slowly added to the solution. Next, 887.80 mg of monobasic potassium phosphate was slowly added to the solution. Deionized water was then added to the solution until a total volume of 1 L was obtained. Once the appropriate mass of dibasic and monobasic potassium phosphate had been added, the buffer solution was mixed using a stirrer at 300 rpm. Finally, the prepared buffer solution was transferred to a 1 L bottle and stored for future experimentation.

Establishing Optimal Excitation Light and PMT Gain Settings

Excitation light and PMT gain were slowly increased to establish the optimization settings. 3 mL blank solutions of deionized water and potassium phosphate buffer were prepared in a plastic or glass cuvette and loaded into the instrument. The light source was turned on for 10 seconds, signal measures were collected and recorded, and turned off for 10 seconds through LabVIEW. This process was repeated for 4 trials. Excitation lights of 0.5, 1.0, 2.0, 3.0, 4.0, and 5.0 V were tested at PMT gains of 0.5, 0.6, 0.7, 0.8, 0.9, 1.0, and 1.1 V (S3-4). Results of these tests were visualized in MATLAB. The PMT was found to saturate at approximately 2.4 V. For the majority of experiments, an excitation light of 3.0 V and PMT gain of 0.6 V were employed to prevent photobleaching and utilize the dynamic range of the instrument.

Establishing Baseline Background Signal Associated with Plastic and Glass Cuvettes

A glass cuvette was found to result in lower background compared to a plastic cuvette (S5). Empty, 3 mL deionized water blank, and 3 mL potassium phosphate buffer blank cuvettes were prepared. The light source was turned on for 10 seconds, signal measurements were collected and recorded, and turned off through LabVIEW. Only one trial was performed during this diagnostic testing. Results of this test were visualized in MATLAB.

Establishing Instrument Functionality for Detecting NADPH in Free Solution

2 mL of 0.840 mM NADPH stock solution was prepared using 2 mL of potassium phosphate buffer and 1.40 mg of NADPH. The stock was then diluted to make 10 mL of 0.1 mM using 1.191 mL of stock solution and 8.809 mL of potassium phosphate buffer. Solutions were then prepared in plastic cuvettes ranging from 0.1 mM to 97.7 nM decreasing by 2-fold each time.

The 3 mL samples were then individually loaded into the instrument. The light source was turned on for 10 seconds, signal measures were collected and recorded, and turned off for 10 seconds through LabVIEW. This process was repeated for 4 trials. The deionized water blank was first tested. Testing then continued in a descending manner of NADPH concentrations.

2-Fold Direct Dilutions from 0.01 mM NADPH Stock Solution

2 mL of 0.966 mM NADPH stock solution was prepared using 2 mL of potassium phosphate buffer and 1.61 mg of NADPH. This stock solution was then diluted to make 10 mL of 0.01 mM using 0.104 mL stock solution and 9.896 mL of potassium phosphate buffer. Solutions were then prepared in plastic cuvettes ranging from 0.01 mM to 0.61 nM decreasing by 2-fold each time resulting in a total of 15 dilutions. Solutions were then transferred to a well cleaned glass cuvette for fluorescence testing.

The 3 mL samples individually were then loaded into the instrument. Excitation light and PMT gain were set in LabVIEW to 3.0 V and 0.6 V, respectively. The light source was turned on for 10 seconds, signal measurements were collected and recorded, and the light source was turned off for 10 seconds through LabVIEW. This process was repeated for 4 trials. The potassium phosphate buffer blank was first tested. Testing then continued in an ascending manner of NADPH concentrations.

2-Fold Direct Dilutions from 0.1 mM NADPH Stock Solution

2 mL of 0.840 mM NADPH stock solution was prepared using 2 mL of potassium phosphate buffer and 1.40 mg of NADPH. The stock was then diluted to make 10 mL of 0.1 mM using 1.191 mL of stock solution and 8.809 mL of potassium phosphate buffer. Solutions were then

prepared in plastic cuvettes ranging from 0.1 mM to 0.61 nM decreasing by 2-fold each time, resulting in a total of 15 dilutions. Solutions were then transferred to a well cleaned glass cuvette for fluorescence testing.

The 3 mL samples were then individually loaded into the instrument. Excitation light and PMT gain were set in LabVIEW to 3.0 V and 0.6 V, respectively. The light source was turned on for 5 seconds, signal measurements were collected and recorded 1 second after the light was turned on, and the light source was turned off for 5 seconds through LabVIEW. This process was repeated for 4 trials. The potassium phosphate buffer blank was tested first, and testing then proceeded in an ascending manner of NADPH concentrations.

End Matter

Author Contribution and Notes

CVA: Literature review to find values for NADPH and neutrophil concentrations in MEF; calculation to establish NADPH concentrations in AOM and OME; literature review to determine extinction coefficient and quantum efficiency of NADPH; calculation to determine the optimal lens for instrument; design of LabVIEW virtual instrument; preliminary experimentation to determine optimal excitation light intensity and PMT gain settings; literature review into NADPH degradation kinetics and oxygen content of MEF; calculations for direct dilutions; stock solution and direct dilution preparation for experimentation.

LAP: Design of custom emission filter holder; LabVIEW set-up, installation, and troubleshooting; design of LabVIEW virtual instrument; establishment of optimal excitation light and PMT gain settings; establishment of background associated with glass and plastic cuvettes; literature review into NADPH degradation kinetics and oxygen content of middle ear fluid; creation of potassium phosphate buffer; running instrument on NADPH samples, measuring and recording data during experimentation; statistical analysis, data analysis and visualization in MATLAB.

ET: Literature review to find values for NADPH and neutrophil concentrations in MEF; calculation to establish NADPH concentrations in AOM and OME; literature review to determine extinction coefficient and quantum efficiency of NADPH; calculation to determine the optimal lens for instrument; design of the physical optical instrument; preliminary experimentation to determine optimal excitation light intensity and PMT gain settings; design of cuvette holder; literature review into NADPH degradation kinetics and oxygen content of MEF; calculations for direct dilutions; stock solution and direct dilution preparation for experimentation.

DW: Design of custom emission filter holder; calculation to establish optimal component specifications and instrument configuration, physical optical instrument design, construction, and troubleshooting; design of cuvette holder; preliminary experimentation to determine optimal excitation light intensity and PMT gain settings; literature review into NADPH degradation kinetics, phosphate buffer fluorescence, and oxygen content of MEF; calculations for direct dilutions; stock solution and direct dilution preparation for experimentation.

Acknowledgements

Dr. William Guilford, Capstone Project Advisor. Dr. Timothy Allen and Dr. Shannon Barker, Capstone Professors. Noah Perry, Natasha Claxton, and Zehra Demir, Capstone Teaching Assistants.

References

1. Schilder, A. G. M. *et al.* Otitis media. *Nat Rev Dis Primers* **2**, 1–18 (2016).

2. Isaacson, J. E. & Vora, N. M. Differential Diagnosis and Treatment of Hearing Loss. *afp* **68**, 1125–1132 (2003).

3. Harmes, K. M. *et al.* Otitis Media: Diagnosis and Treatment. *afp* **88**, 435–440 (2013).

4. Impairments, N. R. C. (US) C. on D. D. for I. with H., Dobie, R. A. & Hemel, S. V. *Hearing Loss in Children*. *Hearing Loss: Determining Eligibility for Social Security Benefits* (National Academies Press (US), 2004).

5. Pichichero, M. E. & Poole, M. D. Assessing Diagnostic Accuracy and Tympanocentesis Skills in the Management of Otitis Media. *Archives of Pediatrics & Adolescent Medicine* **155**, 1137–1142 (2001).

6. Singh, H. *et al.* Errors of Diagnosis in Pediatric Practice: A Multi-Site Survey. *Pediatrics* **126**, 70–79 (2010).

7. Tong, S., Amand, C., Kieffer, A. & Kyaw, M. H. Trends in healthcare utilization and costs associated with acute otitis media in the United States during 2008–2014. *BMC Health Serv Res* **18**, 318 (2018).

8. Inventions of the Year: UMD, JHU Researchers Develop AI-Enhanced Digital Otoscope for Diagnosing Pediatric Ear Disease. *Division of Research* https://research.umd.edu/articles/inventions-year-umd-jhu-researchers-develop-ai-enhanced-digital-otoscope-diagnosing | https://research.umd.edu/ (2022).

9. Ji, Y. B. *et al.* Terahertz otoscope and potential for diagnosing otitis media. *Biomed Opt Express* **7**, 1201–1209 (2016).

10. Mittal, R. *et al.* Role of innate immunity in the pathogenesis of otitis media. *Int J Infect Dis* **0**, 259–267 (2014).

11. Elbistanli, M. S. *et al.* The Predictive Value of Neutrophil-Lymphocyte and Platelet-Lymphocyte Ratio for the Effusion Viscosity in Otitis Media With Chronic Effusion. *Journal of Craniofacial Surgery* **28**, e244 (2017).

12. Nassif, P. S., Simpson, S. Q., Izzo, A. A. & Nicklaus, P. J. Interleukin-8 Concentration Predicts the Neutrophil Count in Middle Ear Effusion. *The Laryngoscope* **107**, 1223–1227 (1997).

13. Nguyen, G. T., Green, E. R. & Mecsas, J. Neutrophils to the ROScue: Mechanisms of NADPH Oxidase Activation and Bacterial Resistance. *Front Cell Infect Microbiol* **7**, 373 (2017).

14. Xie, N. *et al.* NAD+ metabolism: pathophysiologic mechanisms and therapeutic potential. *Sig Transduct Target Ther* **5**, 1–37 (2020).

15. Magnani, F. & Mattevi, A. Structure and mechanisms of ROS generation by NADPH oxidases. *Current Opinion in Structural Biology* **59**, 91–97 (2019).

16. Winterbourn, C. C., Kettle, A. J. & Hampton, M. B. Reactive Oxygen Species and Neutrophil Function. *Annual Review of Biochemistry* **85**, 765–792 (2016).

17. NAD metabolism and mitogen stimulation of human lymphocytes - ScienceDirect. https://www.sciencedirect.com/science/article/abs/pii/0014482785901892.

18. Enzyme Activities Leading to NAD Synthesis in Human Lymphocytes - ScienceDirect. https://www.sciencedirect.com/science/article/abs/pii/S0003986100918885.

19. Blacker, T. S. & Duchen, M. R. Investigating mitochondrial redox state using NADH and NADPH autofluorescence. *Free Radic Biol Med* **100**, 53–65 (2016).

20. Haid, E., Lehmann, P. & Ziegenhorn, J. *The Molar Absorption Coefficients of ß-Nicotinamide- Adenine Dinucleotide*. *Quality Control in Clinical Chemistry* 235–240 (De Gruyter, 2014).

21. Wu, J. T., Wu, L. H. & Knight, J. A. Stability of NADPH: effect of various factors on the kinetics of degradation. *Clin Chem* **32**, 314–319 (1986).

22. L-b-NADPH CAS No. 2646-71-1 Roche. http://www.sigmaaldrich.com/.

23. Study of middle ear fluid pH and pepsinogen 1 level in childhood otitis media. https://www.jstage.jst.go.jp/article/shonijibi/32/1/32_47/_article.

24. Middle Ear Gas Composition in Pathologic Conditions: Mass Spectrometry in Otitis Media with Effusion and Atelectasis. *Ann Otol Rhinol Laryngol* **106**, (1997).

Supplement

(A) **(B)**

Supplement 1: Photomultiplier Tube and Emission Filter Holder AutoCAD Design. (A) *The first panel shows the AutoCAD design for the photomultiplier tube holder. (B) The second panel shows the AutoCAD design for the emission filter holder. The top side of this holder connects to the left side of the photomultiplier tube holder.*

(A) **(B)**

Supplement 2: Cuvette Holder AutoCAD Design*. The above AutoCAD design shows the cuvette holder that was used to load samples into the instrument for experimentation. Use of a glass cuvette required that the inner width of the holder be increased in size to accommodate the new cuvette. (A) The first panel shows an angled view of the cuvette holder. (B) The second panel shows a view of a cuvette holder from front with the hidden edges visible.*

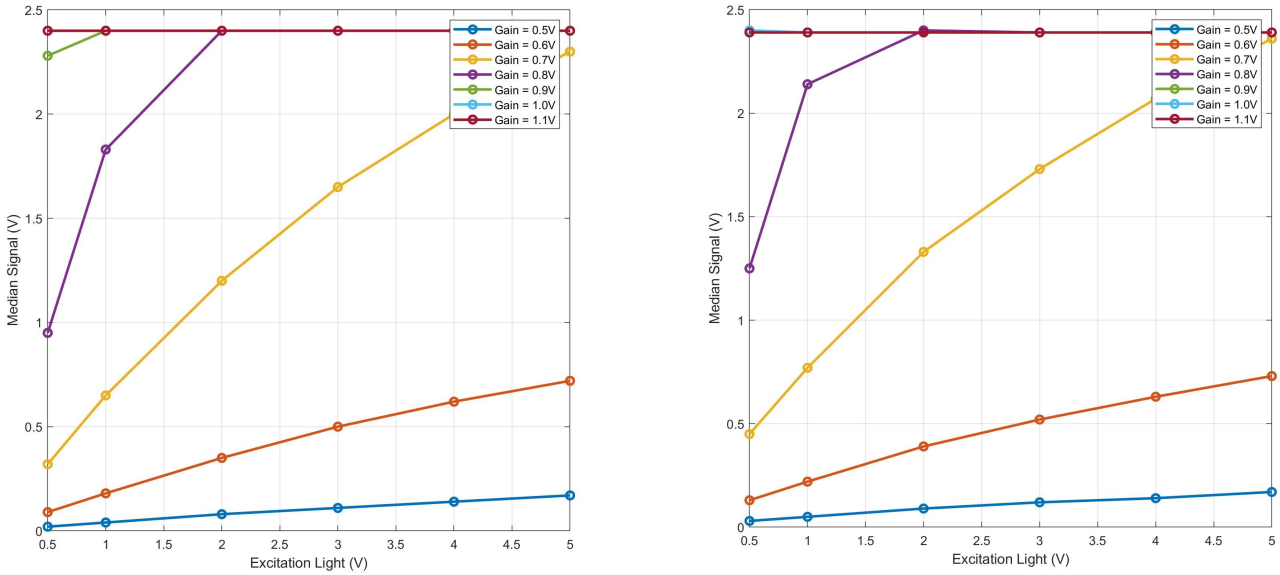

(A) **(B)**

Supplement 3: Excitation Light and PMT Gain Optimization for Deionized Water and Potassium Phosphate Buffer Blanks in Plastic Cuvette. (A) *The first panel shows the median signal at PMT gains of 0.5, 0.6, 0.7, 0.8, 0.9, 1.0, and 1.1 V plotted against excitation lights ranging from 0.5, 1.0, 2.0,0, 4.0, and 5.0 V for a deionized water blank in a plastic cuvette.* ***(B)*** *The second panel shows the median signal at PMT gains of 0.5, 0.6, 0.7, 0.8, 0.9, 1.0, and 1.1 V plotted against excitation lights ranging from 0.5, 1.0, 2.0,0, 4.0, and 5.0 V for a potassium phosphate buffer blank in a plastic cuvette.*

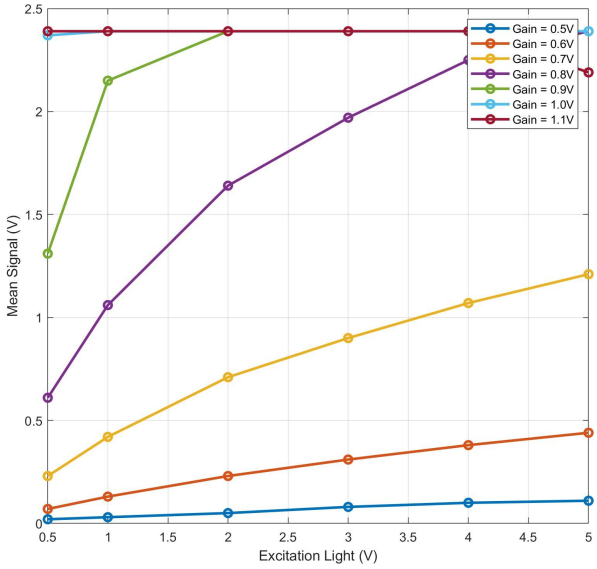

Supplement 4: Excitation Light and PMT Gain Optimization for Potassium Phosphate Buffer in Glass Cuvette. *The above panel shows the mean signal at PMT gains of 0.5, 0.6, 0.7, 0.8, 0.9, 1.0, and 1.1 V plotted against excitation lights ranging from 0.5, 1.0, 2.0, 3.0, 4.0, and 5.0 V for a potassium phosphate buffer blank in a glass cuvette.*

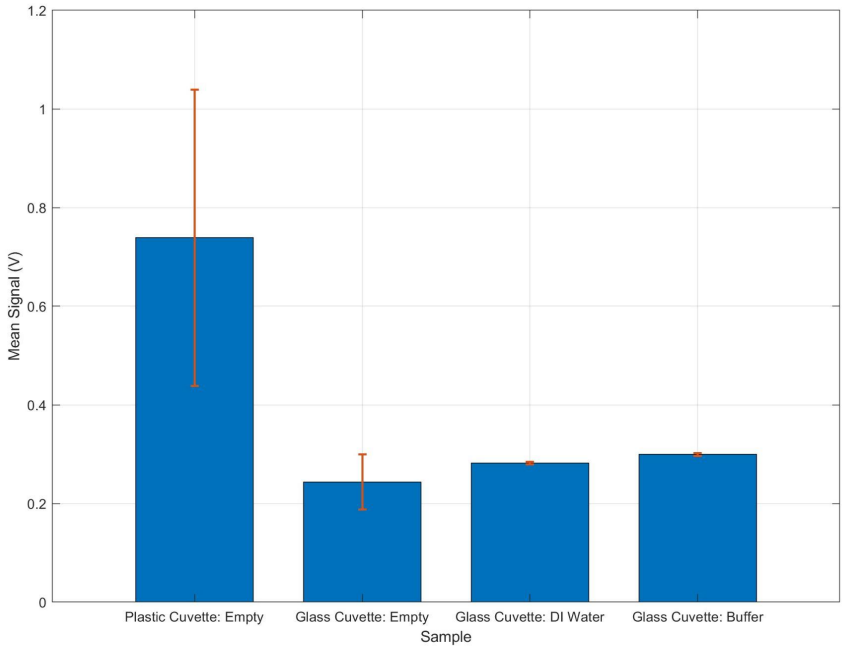

Supplement 5: Establishing Baseline Background Levels of Plastic and Glass Cuvette. *The above panel shows the mean signal for empty plastic and glass cuvettes containing 3 mL of deionized water or potassium phosphate buffer. Standard deviation was calculated for each sample and plotted as error bars. An unpaired, two-sample t-test was performed on the raw signal data for the empty plastic and glass cuvettes. A statistically significant decrease (p-value ≅ 0) in background was found for the glass cuvette relative to the plastic cuvette.*